Korea-Australia Rheology Journal
Vol. 17, No. 3, September 2005 pp. 131-140

Direct numerical simulations of viscoelastic turbulent channel flows at high drag reduction

Kostas D. Housiadas and Antony N. Beris*
Department of Chemical Engineering, University of Delaware Newark, Delaware 19716, USA
(Received, April 28, 2005)

Abstract

In this work we show the results of our most recent Direct Numerical Simulations (DNS) of turbulent viscoelastic channel flow using spectral spatial approximations and a stabilizing artificial diffusion in the viscoelastic constitutive model. The Finite-Elasticity Non-Linear Elastic Dumbbell model with the Peterlin approximation (FENE-P) is used to represent the effect of polymer molecules in solution. The corresponding rheological parameters are chosen so that to get closer to the conditions corresponding to maximum drag reduction: A high extensibility parameter (60) and a moderate solvent viscosity ratio (0.8) are used with two different friction Weissenberg numbers (50 and 100). We then first find that the corresponding achieved drag reduction, in the range of friction Reynolds numbers used in this work (180-590), is insensitive to the Reynolds number (in accordance to previous work). The obtained drag reduction is at the level of 49% and 63%, for the friction Weissenberg numbers 50 and 100, respectively. The largest value is substantially higher than any of our previous simulations, performed at more moderate levels of viscoelasticity (i.e. higher viscosity ratio and smaller extensibility parameter values). Therefore, the maximum extensional viscosity exhibited by the modeled system and the friction Weissenberg number can still be considered as the dominant factors determining the levels of drag reduction. These can reach high values, even for of dilute polymer solution (the system modeled by the FENE-P model), provided the flow viscoelasticity is high, corresponding to a high polymer molecular weight (which translates to a high extensibility parameter) and a high friction Weissenberg number. Based on that and the changes observed in the turbulent structure and in the most prevalent statistics, as presented in this work, we can still rationalize for an increasing extensional resistance-based drag reduction mechanism as the most prevalent mechanism for drag reduction, the same one evidenced in our previous work: As the polymer elasticity increases, so does the resistance offered to extensional deformation. That, in turn, changes the structure of the most energy-containing turbulent eddies (they become wider, more well correlated, and weaker in intensity) so that they become less efficient in transferring momentum, thus leading to drag reduction. Such a continuum, rheology-based, mechanism has first been proposed in the early 70s independently by Metzner and Lamley and is to be contrasted against any molecularly based explanations.

Keywords : turbulence, DNS, FENE-P, drag reduction, viscoelasticity, dilute polymer solutions, extensional viscosity, channel flow

1. Introduction

The phenomenon of polymer-induced drag reduction has fascinated the polymer rheology research community, from the time of its discovery (Mysels, 1949; Toms, 1949) to our days (Dodge and Metzner, 1959; Hershey and Zakin, 1967; Lumley, 1969; Seyer and Metzner, 1969; Virk, 1975; Luchik and Tiederman, 1988; Tanner, 2000). This phenomenon describes the effect that relatively small quantities (as small as of the order of ppm by weight) of a high molecular weight polymer have in reducing the turbulent drag when added to a low molecular weight solvent, such as water or crude oil. Typical exploitation of such an effect is to significantly decrease the skin friction factor in turbulent flows through pipes (as much as 70-75%) leading to applications such as in facilitating the oil transfer through the Alaskan pipeline. However, despite the fact that considerable experimental results are now available, theoretical a-priori analyses are considerably lagging behind. The mostly accepted mechanism (but not universally!) was undoubtedly that due to molecular stretching in the radial flow patterns in turbulent flows proposed independently by Lumley and Metzner (Lumley, 1969; Seyer and Metzner,

*Corresponding author: beris@che.udel.edu

1969) albeit it was Metzner (Seyer and Metzner, 1969) who first clearly identified the role of the high extensional deformation rates and the high resistance to stretching as the more specific causes to drag reduction.

During the last decade many attempts have been made to theoretically understand its nature and the underlying mechanisms thanks to Direct Numerical Simulations (DNS) (Sureshkumar *et al.*, 1997; Dimitropoulos *et al.*, 1998; 2001; De Angelis *et al.*, 2002; Sibilla and Baron, 2002; Housiadas and Beris, 2003; Min *et al.*, 2003; Housiadas *et al.*, 2005). Those are large-scale turbulent computations (therefore, time-dependent and three-dimensional) similar to the ones carried out for Newtonian fluids (Orszag and Kells, 1980; Moin and Kim, 1980) but also accounting for the presence of viscoelasticity.

Viscoelastic simulations are much more demanding than Newtonian simulations. First, they involve more dependent variables in order to model the presence of viscoelasticity in the flow. Viscoelasticity is typically modeled implicitly using one (or more) internal structural parameters in terms of which the molecular deformation is modeled and with respect to which the viscoelastic extra stress (i.e. the contribution of the viscoelasticity to the fluid stress) is expressed (Bird *et al.*, 1997a; Beris and Edwards, 1994; Tanner, 2000). Although the most accurate expressions involve microscopic models that require following individual molecules (using, for example, kinetic theory---see Bird *et al.*, 1997b) usually continuum models which only approximate the evolution of few molecular statistics (typically the second moment of the end-to-end distribution function, represented by a second order nonnegative definite tensor, the conformation tensor **c**) are fairly adequate to present semi-quantitatively the flow behavior (Beris and Edwards, 1994)---even quantitatively, if we allow a renormalization (adjustment) of the model parameters from their microscopically estimated values.

In the case of dilute polymer solutions, the Finite-Elasticity Non-Linear Elastic Dumbbell model with the Peterlin approximation (FENE-P) has proven to be fairly accurate in providing estimated of both the shear and (especially) the extensional rheological behavior (Leal, 1990; Tanner, 2000). Note that albeit discrepancies may be observed when one compares directly the FENE-P against the microscopic (FENE) model predictions (Keunings, 1997) most of those disappear after a suitable rescaling of the model parameters (Van Heel *et al.*, 1998; Gupta *et al.*, 2004). Also note that to adequately represent the effects of polymer additives to turbulent flow it is not adequate to simply utilize a generalized Newtonian (for example, power law) description of the modified by the polymer system's rheology (which would have avoided the solution of additional constitutive relations): Such an approach has only produced minor drag reduction effects (den Toonder *et al.*, 1995; Orlandi, 1995).

The main difficulty of performing the viscoelastic simulations does not however come from just the presence of more variables. Rather it primarily arises because of the challenges presented in numerically integrating the corresponding set of evolution equations for the internal variables at the high Weissenberg numbers required in the simulations to achieve a sizeable drag reduction. In fact, the earliest approach (using an Oldroyd-B constitutive model) failed due to numerical instabilities (Maulik, 1989). A breakthrough took place in 1997 when an artificial diffusivity was employed in the constitutive model (FENE-P) to allow for the numerical calculation of an adequately smooth conformation field to be resolved in the simulations (Sureshkumar *et al.*, 1997) based on some earlier work on the analysis of the effect of diffusion in the numerical time integration of viscoelastic equations (Sureshkumar and Beris, 1995). The 1997 pioneering viscoelastic DNS work was followed from several others (Dimitropoulos *et al.*, 1998; 2001; De Angelis *et al.*, 2002; Sibilla and Baron, 2002; Housiadas and Beris, 2003; Min *et al.*, 2003; Housiadas and Beris, 2004a; 2004b; Housiadas *et al.*, 2005).

In all of the above mentioned works the solution to the constitutive equation is made possible through the use of a numerical diffusion which is either added explicitly (typically in high order spectral approximations) or implicitly thought the use of low order (upwind) formulations. What has not been very clearly stated so far is the fact (as we believe now) that the need for artificial diffusion arises not just in order to stabilizing the numerical integration of the constitutive model. Rather, the primary role of the numerical diffusion added to the evolution equation of the internal structural (conformation) variable is considered to be that of smoothening up the conformation field so that it can be represented with a finite resolution, i.e. so that in Fourier space the magnitude of the higher modes remains finite and does not blow up in time. This blow up is unavoidable if no diffusion is used due to the chaotic nature of the turbulent flow field which it driving the evolution of the conformation. This is not new, but rather common to all advection effects in the presence of a chaotic flow, as it has been well documented in similar situations associated with the advection if passive scalars in the presence of turbulence (Fox, 2003). In fact it is for this reason that an additional artificial diffusion needs to be used when solving for the advection-diffusion equation for a passive scalar in turbulent flow when the molecular diffusion alone is too small (corresponding to molecular Schmidt numbers of the order or greater than 1) (Fox, 2003).

We believe that, exactly parallel to those passive scalar observations, the addition of numerical diffusivity to viscoelastic equations is also necessary in order to preserve the finite magnitude of the high frequency Fourier modes, as the conformation structures in a chaotic flow regime

have a tendency to become, in the absence of a cross-streamline conformational diffusion, more and more fine. The challenge of course is to simultaneously avoid adding too much diffusion, in which case one risks to pollute even the dynamics of larger scale features. For that reason, and based on previous passive scalar analysis work in Newtonian turbulent flows, and, more specifically, the analysis of mixing (Fox, 2003), the use of numerical diffusivity corresponding to a numerical Schmidt number similar to the value of 0.4 used in those flow simulations is also advocated here (a value of 0.2-0.3 is used in this work). The (slightly) smaller value has been found necessary in order to account for additional destabilizing effects associated with the solution of viscoelastic constitutive equations arising from the stretching present in those equations as well as the tensorial character that makes especially critical the preservation of nonnegative definiteness (Joseph, 1989).

The presence of eddies completely transforms the balance of various terms in the constitutive equation which now becomes, except for a very thin boundary layer, extension dominated. The main outcome of the DNS works so far has therefore been the ample supply of evidence in favor of an extensional viscosity thickening-driven drag reduction mechanism. As the eddies form at the wall, they see with viscoelasticity increased resistance due to the predominantly extensional character of the velocity deformation and the enhanced resistance to extensional deformation offered by polymers, exactly as foresaw by Metzner (Seyer and Metzner, 1969) and also independently postulated by Lumley (1969). As a result, with increasing viscoelasticity we see the eddies to be larger in size, of smaller magnitude and more sluggish; therefore becoming less effective in transferring momentum from the wall, thus resulting in drag reduction.

However, in the above mentioned works, the degree of viscoelasticity in the flow, as characterized, for example, by the maximum extensional viscosity and the friction Weissenberg number, was not sufficiently high to reach high levels of drag reduction. Albeit the values of drag reduction reached increased steadily, from about 30% of the earlier work (Sureshkumar *et al.*, 1997) to about 38% later on with the FENE-P model (Housiadas and Beris, 2003) and the Giesekus model (Housiadas and Beris, 2004b) there is still need to understand what happens at higher levels of drag reduction. This is exactly what the present work attempts to offer looking at levels as high as 63% by suitably adjusting the model parameters. With this opportunity we should note that some of the drag reduction levels reported in the literature appear to be higher. For example, with the Giesekus model and almost identical conditions to the ones used in (Housiadas and Beris, 2004b) Yu and Kawaguchi (2003) report drag reduction values as high as 53%. However, one should note the use of a lower order method (second order finite differences) in that work; otherwise it has some advantages as it uses a MINMOD scheme for the integration of the constitutive model. Similarly, in the work of Ptasinski *et al.* (2003) drag reduction values using the FENE-P model are reported as high as 66% (using lower solvent viscosity ratios than here). However, there are questions raised due to the use of a lower order finite difference scheme in the shear direction, as well as due to the use of a small computational domain. Thus, the evaluation of high drag reduction with high accuracy methods and the development of consistent convergence studies with respect to mesh resolution and accuracy is still, we believe, an open subject (especially given the complexity of the problem).

2. Governing equations and numerical implementation

The turbulent channel flow simulations are carried out by a pseudospectral numerical algorithm that was originally developed by Beris and Sureshkumar (1996), based on a time-splitting semi-implicit spectral technique similar to that used for the direct numerical simulation of turbulent Newtonian channel flow (Orszag and Kells, 1980; Moin and Kim, 1980; Kim and Moin, 1985). A second order Adams-Bashforth method was used for the explicit update of the non-linear terms and a second order Adams-Moulton scheme for the implicit update of the linear terms. The continuity, momentum and the constitutive model equations for the three-dimensional time-dependent viscoelastic turbulent cannel flows are, in general, given as

$$\nabla\cdot\boldsymbol{v}=0$$

$$\frac{D\boldsymbol{v}}{Dt}=-\nabla p_p+\frac{\beta_0}{Re_{\tau 0}}\nabla^2\boldsymbol{v}+\frac{(1-\beta_0)}{Re_{\tau 0}}\nabla\cdot\tau+\boldsymbol{e}_x$$

$$\frac{\delta\boldsymbol{c}}{\delta t}=-\tau-\alpha We\,\tau\cdot\tau+\frac{D_0^+}{Re_{\tau 0}}\nabla^2\boldsymbol{c}$$

$$\tau=\frac{(f(\boldsymbol{c})\boldsymbol{c}-\boldsymbol{I})}{We},\begin{cases}f(\boldsymbol{c})=\dfrac{L^2}{L^2-trace(\boldsymbol{c})},\ L>0,\ \alpha=0:FENE-P\\ f(\boldsymbol{c})=1,\ \alpha=0:Oldroyd-B\\ f(\boldsymbol{c})=1,\ \alpha>0:Giesekus\end{cases}\qquad(2.1)$$

where β_0 is the ratio of the solvent to the total zero shear-rate viscosity, ∇p_p is the periodic component of the pressure and $\boldsymbol{e}_x$ is the unit vector along the streamwise direction. The viscoelastic constitutive model employed in Eq. (2.1) is a generalization of both the FENE-P and the Giesekus models (Bird *et al.*, 1997a; 1997b; Tanner, 2000), written in terms of an internal structural parameter (Beris and Edwards, 1994) so that one can capture in the same model both finite extensibility (through the extensibility parameter, L) and concentration (through the anisotropic mobility parameter, α) effects. As indicated in Eq. (2.1) both of these equations can be recovered at certain limits. In this work we limit ourselves in examining pure FENE-

P behavior (setting the anisotropic mobility factor to zero) but some comparison against results obtained with the Giesekus model is also offered.

As a consequence of the time integration of these equations using a mixed explicit/implicit time integration, it can then be shown that the velocity $\boldsymbol{v}$ and the conformation tensor $\boldsymbol{c}$, both at the $(n+1)$-th time step, can be written as:

$$\boldsymbol{v}^{n+1}-\boldsymbol{v}^{n}=\frac{\Delta t}{2}[-3(\boldsymbol{v}\cdot\nabla\boldsymbol{v})^{n}+(\boldsymbol{v}\cdot\nabla\boldsymbol{v})^{n-1}] +\frac{(1-\beta_0)\Delta t}{2Re_{\tau 0}}[\nabla\cdot\boldsymbol{\tau}^{n+1}+\nabla\cdot\boldsymbol{\tau}^{n}]-\Delta t\nabla p_p +\frac{\beta_0\Delta t}{2Re_{\tau 0}}[\nabla^2\boldsymbol{v}^{n+1}+\nabla^2\boldsymbol{v}^{n}]+\Delta t\boldsymbol{e}_x \tag{2.2}$$

and

$$\boldsymbol{c}^{n+1}-\boldsymbol{c}^{n}=\frac{\Delta t}{2}[3(-\boldsymbol{v}\cdot\nabla\boldsymbol{c}+\boldsymbol{c}\cdot\nabla\boldsymbol{v}+(\nabla\boldsymbol{v})^{T}\cdot\boldsymbol{c}-\boldsymbol{\tau}-aWe\,\boldsymbol{\tau}\cdot\boldsymbol{\tau})^{n} -(-\boldsymbol{v}\cdot\nabla\boldsymbol{c}+\boldsymbol{c}\cdot\nabla\boldsymbol{v}+(\nabla\boldsymbol{v})^{T}\cdot\boldsymbol{c}-\boldsymbol{\tau}-aWe\,\boldsymbol{\tau}\cdot\boldsymbol{\tau})^{n-1}] +\frac{D_0^{+}\Delta t}{2Re_{\tau 0}}\nabla^2(\boldsymbol{c}^{n+1}+\boldsymbol{c}^{n}) \tag{2.3}$$

respectively, where Δt is the time step size and ∇p_p is calculated from the divergence of the momentum equation which is simply a Poisson equation. The boundary conditions for the pressure Poisson equation are constructed using the influence matrix method (Sureshkumar and Beris, 1995; Beris and Sureshkumar, 1996; Phillips and Soliman, 1991).

The above set of equations leads to an update of the velocity components that is obtained in three stages. First, the calculation of the contribution to the velocity from the inertial terms and the viscoelastic extra stress is performed. The contribution of the inertial terms can be evaluated explicitly from the velocity data obtained at the two previous time steps as they are required in the time-integration scheme. The contribution of the viscoelastic extra stress is evaluated from the conformation tensor using equations 3.1 after it is calculated at the new time step. The detailed procedure can be found in the work of Dimitropoulos *et al.* (1998).

Dimitropoulos *et al.* (1998) reported results obtained (for the first time) with the Giesekus model using the numerical algorithm, which is briefly described in the current paper. In that work, the simulations had been performed for a large value of the mobility factor ($a=0.01$) which corresponds to a low value of the FENE-P extensibility parameter ($L=10$) using an excessive amount of artificial diffusion. From the numerical point of view the Giesekus model appeared more demanding and more difficult to perform the simulations than the FENE-P model. In order to stabilize further the numerical algorithm and eliminate most of the drawbacks of the old algorithm, Housiadas and Beris (2004b) developed an improved algorithm for DNS

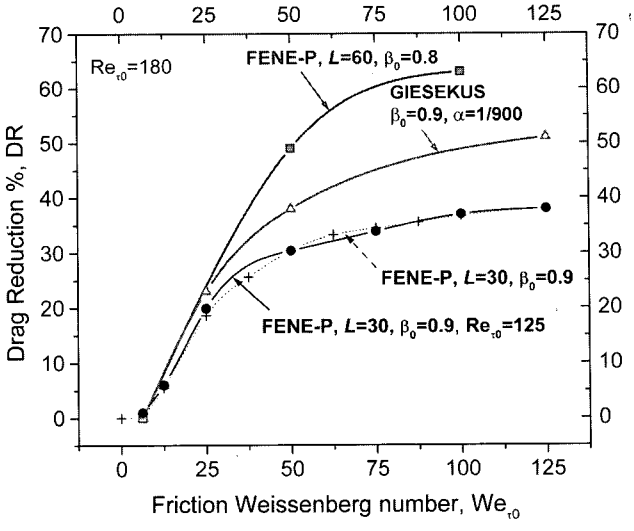

Fig. 1. The achieved drag reduction, through DNS, as a function of the friction Weissenberg number for the FENE-P and the Giesekus constitutive models.

Table 1. Dimensionless numbers (reference values) and other model parameters and their definition

Dimensionless number	Symbol	Definition
Friction Reynolds	$Re_{\tau 0}$	$h^* u_\tau^* / \nu_0^*$
Friction Weissenberg	$We_{\tau 0}$	$\lambda^* u_\tau^{*2} / \nu_0^*$
Viscosity ratio	β_0	$\eta_s^* / (\eta_s^* + \eta_{p0}^*)$
Numerical diffusivity	D_0^+	k^* / ν_0^*
Weissenberg	We	$\lambda^* u_\tau^* / h^*$
Maximum extensibility	L	$R_0^{*2} K^* / (k_\beta^* / T^*)$
Mobility	a	-

in a straight channel. They were able to extend the calculations in the parameter space and reach a drag reduction of about 37.4% for $a=1/900$ and $We_{\tau 0}=50$. In this work we have reached at even higher levels of drag reduction (~51%) for $a=1/900$ and $We_{\tau 0}=125$, see Fig. 1. It is also noted that although for the FENE-P model both the algorithm used here and the one used by Housiadas and Beris (2004b) can give reliable results, for the Giesekus model only the improved algorithm is used.

The corresponding dimensionless numbers and model parameters entering the governing equations and their definitions are given in Table 1, below.

The numerical parameters used in the simulations are reported in detail in Table 2. A high extensibility parameter ($L=60$) and a moderate solvent viscosity ratio ($\beta_0=0.8$) are used with two different high friction Weissenberg numbers ($We_{\tau 0}=50$ and 100). The numerical diffusivity is between 3.25 and 4.5 depending on the simulation conditions. Four different values of the friction Reynolds number are used: 125, 180, 395 and 590, however the results at

Table 2. Numerical values for the dimensionless numbers and the numerical parameters used for DNS. Note that for the domain size and the integration time the computational units of length and time are used defined as the channel half width, h^*, and h^*/u^*, respectively

$Re_{\tau 0}$	$We_{\tau 0}$	β_0	L	Domain size ($L_x \times L_y \times L_z$)	Mesh size ($N_x \times N_y + 1 \times N_z$)	Integration time
180	0	-	-	$9.0 \times 2.0 \times 4.5$	$96 \times 97 \times 96$	40
180	50	0.9	30	$9.0 \times 2.0 \times 4.5$	$96 \times 97 \times 96$	40
180	50	0.8	60	$9.0 \times 2.0 \times 4.5$	$128 \times 129 \times 128$	20
180	100	0.8	60	$9.0 \times 2.0 \times 4.5$	$128 \times 129 \times 128$	20
395	50	0.8	60	$2\pi \times 2 \times \pi$	$192 \times 193 \times 192$	20
395	100	0.8	60	$2\pi \times 2 \times \pi$	$192 \times 193 \times 192$	20
590	100	0.8	60	$2\pi \times 2 \times \pi$	$256 \times 257 \times 256$	20

the lowest friction Reynolds number 125 with the highest Weissenberg number (100) were not reliable due to an eventual loss of convergence of the solution upon further integration in time. The unreliability of the results was further confirmed through comparison to the results obtained at higher Reynolds numbers. The runs at the higher $Re_{\tau 0}$ numbers were indeed performed primarily to ascertain the convergence of the results (at least as far as the predicted drag reduction levels are concerned) with the Reynolds number, as was seen in our previous studies (Housiadas and Beris, 2003; 2004a). Beyond that, in the following, we report primarily detailed results in the following section based on the simulations performed at $Re_{\tau 0}$=180.

3. Results and discussion

First it is instructive to represent roughly the trends on the predicted drag reduction as a function of the zero shear rate friction Weissenberg number, as we move to the new parameter values window $L = 60$ and $\beta_0 = 0.8$ using the FENE-P model. These are offered, calculated using the standard procedure outlined in (Housiadas and Beris, 2004a), in the first figure, Fig. 1, in comparison to previous results obtained either with FENE-P ($L = 30$, $\beta_0 = 0.9$) or Giesekus ($\alpha = 1/900$, $\beta_0 = 0.9$)---the Giesekus model results also include some new data obtained using the improved algorithm developed by Housiadas and Beris (2004b) at $We_{\tau 0} = 125$. Before discussing the results, it is important to comment on the viscoelastic properties of the systems corresponding to those parameter values. In particular, we want to focus to the extensional viscosity, or, rather, in dimensionless form, the Trouton ratio, T, defined as the ratio of the extensional to the zero shear rate viscosity. As a function of the extensional rate, $\dot{\varepsilon}$, and for a uniaxial extensional flow, this is represented by a sigmoid curve (Wedgewood and Bird, 1988). Starting at vanishingly small values of $\dot{\varepsilon}$ from the Newtonian value (3), the Trouton ratio increases steeply for values of $\lambda\dot{\varepsilon}$ of order 1 to eventually asymptote to a maximum value, equal to $2L^2(1-\beta_0)$ for the FENE-P and $2(1-\beta_0)/\alpha$ for the Giesekus model, respectively. For the model parameters investigated in this work ($L = 60$, $\beta_0 = 0.8$) this maximum Trouton ratio has the value of 1440. This is to be contrasted against the value of 180 corresponding to both the Giesekus model ($\alpha = 1/900$ and $\beta_0 = 0.9$) and the FENE-P model ($L = 30$, $\beta_0 = 0.9$) parameter values that were used in previous simulations (with the exception of the Giesekus results at $We_{\tau 0} = 125$ that are new results for the first time reported here) and against the predictions of which the current drag reduction prediction values are compared.

The first thing that it is therefore of interest to notice from Fig. 1 is that the drag reduction curves with respect to the friction Weissenberg number exhibit a similar sigmoid behavior to that of the Trouton ratio with respect to a dimensionless extensional rate. Moreover, the maximum of in the curves correlates well with the maximum Trouton ratio, with some secondary effects emerging from other features of the model. For example, while as we notice above both the Giesekus ($\alpha = 1/900$ and $\beta_0 = 0.8$) and the FENE-P ($L = 30$, $\beta_0 = 0.9$) models predict the same maximum Trouton ratio, the drag reduction reported for the former is significantly higher than the second---this was noticed also in previous works where the two models have been first compared against each other (Dimitropoulos *et al.*, 1998; Housiadas & Beris, 2004b) and can be possibly attributed to the nonzero second normal stress effect present in the Giesekus model, but absent in the FENE-P. However, we see that eventually the maximum extensional viscosity effect dominates the picture and the drag reduction obtained with the new FENE-P parameters is substantially higher than either the Giesekus or previous FENE-P model predicted, reaching as much as 63% for $We_{\tau 0} = 100$. This brings us close to the Maximum Drag Reduction regime, as reported by Virk (1975). Based on the results presented here, we can stipulate that one can get even higher drag reduction, possibly even the maximum drag reduction, should one use model parameters to the FENE-P model that allow for even higher Trouton ratios.

The next figure, Fig. 2 shows a comparison of the mean velocity predictions between various models for different simulation conditions. The many curves reported for the FENE-P ($L = 60$, $\beta_0 = 0.8$, $We_{\tau 0} = 100$) correspond to sim-

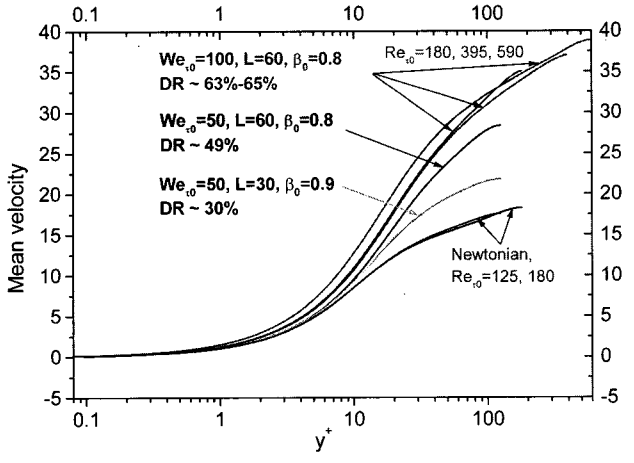

Fig. 2. The mean velocity profile as a function of the distance of the wall in "+" units and semi-logarithmic scale.

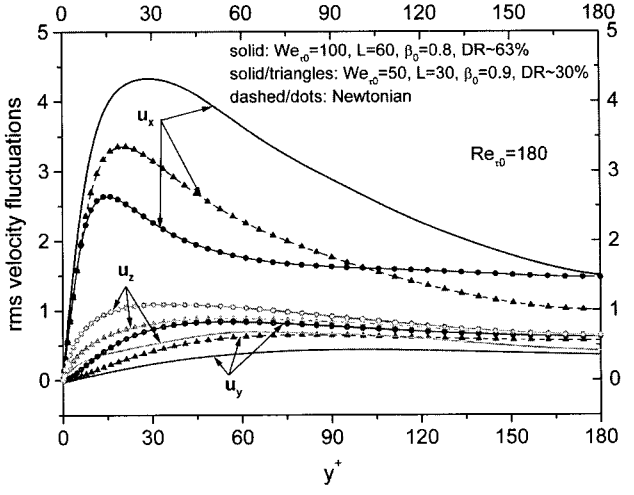

Fig. 3. The rms velocity fluctuations as a function of the distance of the wall in "+" units for three cases: (a) high drag reduction (solid lines), (b) moderate drag reduction (solid lines with triangles) and (c) Newtonian case (solid lines with dots).

ulations conducted at different $Re_{\tau 0}$. The coincidence of the curves accounts for the almost identical predictions for the drag reduction, their insensitivity to the Reynolds number (when the friction Weissenberg number is kept the same) confirming earlier observations at lower drag reduction values (Housiadas and Beris, 2003).

What we see now in conjunction with the predictions from the simulations at the higher Trouton ratio conditions ($L = 60$, $\beta_0 = 0.8$) is a substantial alteration at the log-linear part of the curves in the inertial boundary layer involving both a significant transition region, corresponding to a drastic alteration of the slope, reminiscent of the Virk's asymptote (Virk, 1975) followed by an eventual leveling off, typical to the behavior seen before with dilute polymer systems, but corresponding to substantially higher intercepts, the higher the friction Weissenberg number, the higher the intercept. This behavior is consistent to high drag reduction and it appears consistent to the maximum drag reduction concept---compare Fig. 1 against the experimental data provided in Fig. 9 of (Virk, 1975). This is definitely very reassuring in providing us evidence that we move in the right direction, towards the capability of predicting maximum drag reduction, as we increase the extensional viscosity characteristics of the model.

The fact that we obtain high drag reduction results even with the FENE-P model, a model typically well suited for representing a dilute polymer solution behavior, is consistent to the fact that one can apparently get maximum drag reduction even for such a dilute system, provided the molecular weight of the polymer is high enough (see Table 4 in Virk, 1975). However, we should keep in mind that typically more concentrated systems are the ones that exhibit high and maximum drag reduction---for those systems, one may see significant changes in the details of the velocity profiles and higher statistics versus the current predictions (Vlachogiannis *et al.*, 2003).

Corresponding to the highest drag reduction, the root mean square (rms) values of all the velocity component fluctuations are reported in the next figure, Fig. 3, as a function of the distance from the wall. For comparison purposes, two more cases are also shown there: a viscoelastic one with a moderate drag reduction, and that of a Newtonian fluid. What we observe is that there seems to be a smooth continuation on the trends observed at the moderate drag reduction case as we move to the high drag reduction. Namely, the streamline velocity fluctuations continue to increase (with the maximum shifting further from the wall towards the centerline) whereas those of the other two components continue to decrease.

The rms vorticity fluctuation predictions are to be found in the next figure, Fig. 4, where a comparison against the Newtonian results and a viscoelastic case with a moderate drag reduction is also offered. Here, whereas the trends observed in the streamwise vorticity seem to be smoothly continued and, correspondingly, the rms streamline vorticity values continue to decrease as the drag reduction increases (consistent with the concept of decreasing magnitude of the eddies), there are considerable changes as one goes from moderate to high drag reduction in the behavior of the other rms vorticity components. Most obvious is the case for the rms spanwise component, where one sees a reversal of behavior, with the viscoelastic values higher than even the Newtonian ones. However, one needs to be cautioned of the role of shear thinning as that may be important due to the lower β_0 value for the higher drag reduction case; that can certainly explain higher wall shear rates resulting in higher spanwise vorticity. A more formal analysis, where the effects of the wall shear thinning can be

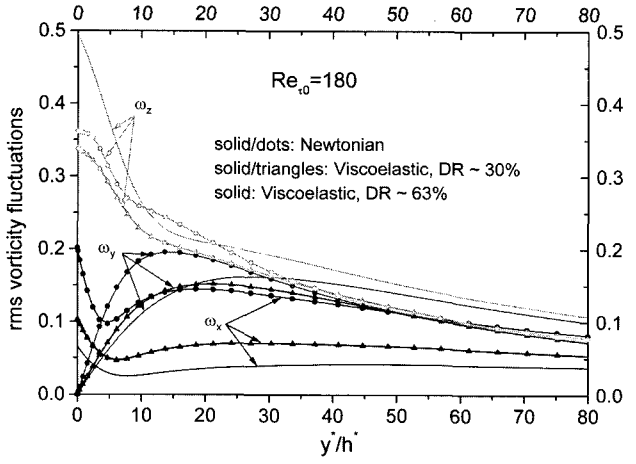

Fig. 4. The rms vorticity fluctuations as a function of the distance of the wall in "+" units for three cases: (a) high drag reduction (solid lines), (b) moderate drag reduction (solid lines with triangles) and (c) Newtonian case (solid lines with dots).

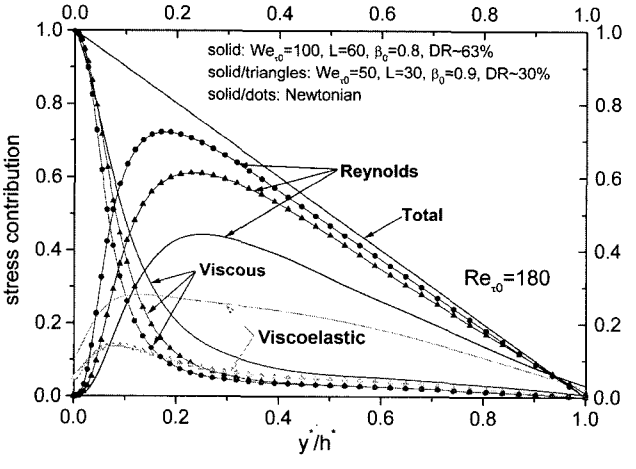

Fig. 5. The various stress contributions to the average total shear stress in the streamwise direction as a function of the distance of the wall in computational units for three cases: (a) drag reduction 63% (solid lines), (b) drag reduction 30% (solid lines with triangles) and (c) Newtonian case (solid lines with dots).

taken into account is still possible, following the procedures outlined in (Housiadas and Beris, 2004a). However, this is not further pursued here in the interest of simplicity.

One of the most important comparisons is certainly that of the Reynolds stress. This is indicated in the next figure, Fig. 5, along with the other contributions to the total mean shear stress, the viscous and viscoelastic. Again, we compare the high against the moderate drag reduction viscoelastic cases and against the Newtonian one.

As we can see there, again it seems to have smooth, continuous, changes in the predictions as the drag reduction increases. Moreover, as far as the Reynolds stress is concerned, this is lowered substantially, but not completely, as viscoelasticity increases with the maximum further moving towards the centerline. On the other hand, the viscous contribution increases modestly, whereas, of course, the viscoelastic one increases substantially, and, for the high drag reduction case, it becomes significant throughout the boundary layer (not just in the viscous and buffer regions). This is a significant qualitative change, perhaps the most important one that we have seen in these high drag reduction simulations.

Finally, these results are to be contrasted against changes in the turbulence structure, a glimpse of which is offered here based on the analysis of the one-dimensional energy spectra. Those are offered in Figs. 6 and 7: in Fig. 6 we

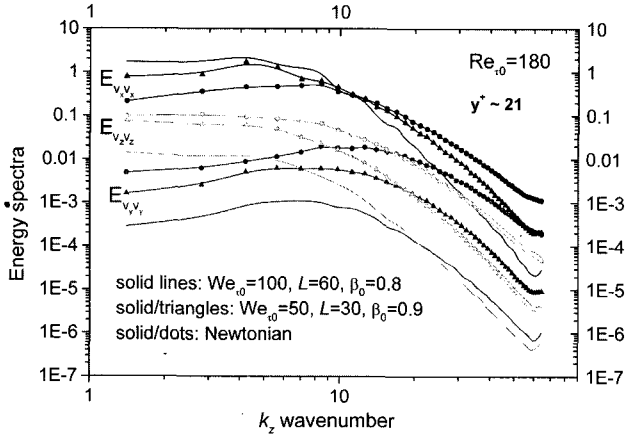

Fig. 6. The one-dimensional energy spectra for the three velocity components as a function of the spanwise wavenumber for three cases: (a) drag reduction 63% (solid lines), (b) drag reduction 30% (solid lines with triangles) and (c) Newtonian case (solid lines with dots).

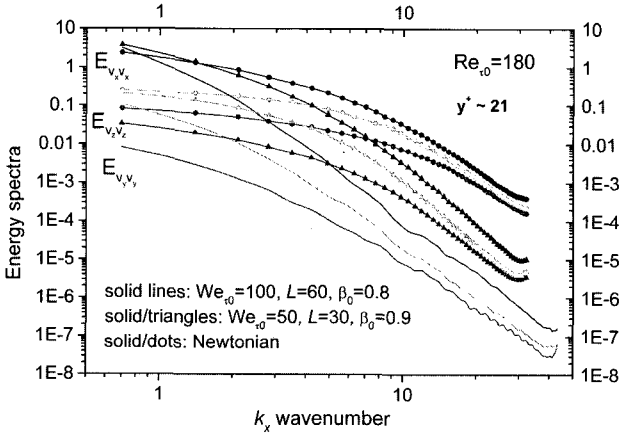

Fig. 7. The one-dimensional energy spectra for the three velocity components as a function of the streamwise wavenumber for three cases: (a) drag reduction 63% (solid lines), (b) drag reduction 30% (solid lines with triangles) and (c) Newtonian case (solid lines with dots).

present the energy spectra for each one of the three velocity components against the spanwise wavenumber, whereas in Fig. 7 against the streamwise one.

The most interesting features are definitely those exhibited by the energy spectra of the streamline velocity component as a function of the spanwise wavenumber (top set of curves in Fig. 6). From there one can see a very significant transition that takes place as viscoelasticity sets in: The low wavenumber contributions increase in intensity, whereas the high ones decrease. This is consistent with the strengthening of the streaky structures and their widening in the spanwise direction, also seen to correlate well with drag reduction (Virk, 1975; Luchik and Tiederman, 1988; Sureshkumar *et al.*, 1997). In contrast, for all the other velocity component spectra and for both behaviors, i.e. with respect to either the spanwise or streamwise wavenumbers (but also for the spanwise velocity spectra with respect to the streamwise wavenumber) we see a uniformly decreasing spectrum.

4. Conclusions

What we have seen here is a successful DNS simulation of high drag reduction viscoelastic cases (close to, albeit not at maximum). For most of the data we see a continuous transition from moderate to high drag reduction, with consistent changes in all primary variables, along the lines (but more enhanced) of the changes observed at moderate drag reduction values. Furthermore, it is characteristic that the Reynolds stress is still quite significant even when the drag reduction reaches 63%. This casts some doubt whether a zero Reynolds stress is a necessary prerequisite for maximum drag reduction---note here that the Reynolds stress may still go to zero for a concentrated or heavily aggregated system, as those effects are not taken into account in the present model; these are more consistent with the conditions under which such significant decrease in the Reynolds stress is observed experimentally (Vlachogiannis, 2003). Moreover, some serious questions are placed on the validity of certain simplified models that have been recently proposed for maximum drag reduction (L'vov *et al.*, 2004) and are based heavily not only on a zero Reynolds stress assumption, but other assumptions that upon closer scrutiny are also not in accordance to the DNS results.

Simultaneously, we need to note here that significant departures from the trends observed at more moderate drag reductions have also been observed in these high drag reduction DNS simulations. In particular, we saw for the first time significant variations in the log-linear law of the wall for the average streamwise velocity component. We have also noticed an enhancement (instead of a decrease) for the RMS vorticity fluctuations. Finally, we noticed the viscoelastic contributions to the average shear stress to remain significant even in the inertial section of the boundary layer. All these point out that significant qualitative changes are taking place in the turbulent structure as we move into regimes with a stronger viscoelastic response. Those changes are captured by the FENE-P model and the DNS simulations and are believed to be responsible eventually for the high drag reduction. This is consistent with a strengthening of the Lumley-Metzner mechanism for drag reduction where the eddies formation and evolution is even more affected now by viscoelasticity, even in the inertial region, as opposed to just at the buffer layer, a key finding of our earlier work that was limited to more modest degrees of drag reduction. The added significance to the large structures cannot be overemphasized. The dominance of the large structures in viscoelastic turbulence is also consistent to previous findings based on Karhunen-Loeve analysis (Housiadas *et al.*, 2005) as well as the analysis of coherent structures (Stone *et al.*, 2004). However, we need to repeat again the caution offered before: we are modeling here primarily a dilute polymer system. In particular, no concentration effects are taken particularly into account (certainly not those that result in a nonzero second normal stress, as this is captured in the Giesekus model) but certainly, and most importantly, we did not have a mechanism to capture in any way any aggregation phenomena that have in many occasions observed to occur in association with turbulent flows of concentrated amphiphilic and anionomer polymer systems (Vlachogiannis *et al.*, 2003) which result in significant anisotropies and inhomogeneities in the system.

Finally, the strengthening of the correlations and the thickening of the streaky structures needs to be underlined, which casts serious doubts on the validity of any results obtained with a minimum computational domain size; if not anything else, the domain size needs to be increased and the convergence of the results to be checked when significant viscoelasticity if present. This is only one of the many requirements (in addition to an adequate integration of the equations, a small enough diffusivity and adequate mesh resolution) that make viscoelastic DNS turbulent simulations very hard to perform even with today's computational resources.

Acknowledgments

The authors would like to acknowledge the financial support provided by DARPA, Grant No.: MDA972-01-1-0007. We are grateful to the National Center for Supercomputing Applications (NCSA) for providing the extensive computational resources needed for this work through as Alliance proposal grand MCA96N005.

References

Beris, A.N. and B.J. Edwards, 1994, *Thermodynamics of Flowing Systems*, Oxford Univ. Press, New York.

Beris, A.N. and R. Sureshkumar, 1996, Simulation of time-dependent viscoelastic channel Poiseuille flow at high Reynolds numbers, *Chemical Engineering Science* **51**, 1451-1471.

Bird, R.B., R.C. Armstrong and O. Hassager, 1987a, *Dynamics of Polymeric Fluids, vol. 1, 2nd ed.* John Wiley and Sons, New York.

Bird, R.B., C.F. Curtiss, R.C. Armstrong and O. Hassager, 1987b, *Dynamics of Polymeric Fluids, vol. 2, 2nd ed.* John Wiley and Sons, New York.

De Angelis, E., C.M. Casciola and R. Piva, 2002, DNS of wall turbulence: dilute polymers and self-sustaining mechanisms, *Computers & Fluids* **31**, 495-507.

Den Toonder, J.M.J., F.T.M. Nieuwstadt and G.D.C. Kuiken, 1995, The role of elongational viscosity in the mechanism of drag reduction by polymer additives, *Appl. Sci. Res.* **54**, 95-123.

Dimitropoulos, C.D., R. Sureshkumar and A.N. Beris, 1998, Direct numerical simulation of viscoelastic turbulent channel flow exhibiting drag reduction: effect of the variation of rheological parameters, *J. Non-Newtonian Fluid Mech.* **79**, 433-468.

Dimitropoulos, C.D., R. Sureshkumar, A.N. Beris and R.A. Handler, 2001, Budgets of Reynolds stress, turbulent kinetic energy and vorticity production in the turbulent channel flow of a dilute polymer solution, *Phys. Fluids* **13**, 1016-1027.

Dodge, D.W. and A.B. Metzner, 1959, Turbulent flow of Non-Newtonian systems, *A.I.Ch.E. J.*, **5**, 189-203.

Fox, R.O., 2003, *Computational Models for Turbulent Reacting Flows*, Cambridge University Press, New York.

Gupta, V.K., R. Sureshkumar and B. Khomami, 2004, Polymer chain dynamics in Newtonian and viscoelastic turbulent channel flows, *Phys. Fluids* **16**, 1546-1566.

Hershey, H.C. and J.L. Zakin, 1967, Molecular approach to predicting the onset of drag reduction in the turbulent flow of dilute polymer solutions, *Chem. Eng. Sci.* **22**, 1847-1857.

Housiadas, K.D. and A.N. Beris, 2003, Polymer-induced drag reduction: Effects of the variations in elasticity and inertia in turbulent viscoelastic channel flow, *Phys. Fluids* **15**, 2369-2384.

Housiadas, K.D. and A.N. Beris, 2004a, Characteristic scales and drag reduction evaluation in turbulent channel flow of non-constant viscosity viscoelastic fluids, *Phys. Fluids* **16**, 1581-1586.

Housiadas, K.D. and A.N. Beris, 2004b, An efficient fully implicit spectral scheme for DNS of turbulent viscoelastic channel flow, *J. Non-Newtonian Fluid. Mech.* **122**, 243-262.

Housiadas, K.D., A.N. Beris and R.A. Handler, 2005, Viscoelastic effects on higher order statistics and on coherent structures in turbulent channel flow, *Phys. Fluids* **17**, 035106 (20 pages).

Joseph, D.D., 1990, *Fluid Dynamics of Viscoelastic Liquids*, Springer-Verlag, New York.

Keunings, R., 1997, On the Peterlin approximation for finitely extensible dumbbells, *J. Non-Newtonian Fluid Mech.* **68**, 85-100.

Kim, J. and P. Moin, 1985, Application of a fractional-step method to incompressible Navier-Stokes equations, *J. Comput. Phys.* **59**, 308-323.

Leal, L.G., 1990, Dynamics of dilute polymer solutions, in: *Structure of Turbulence and Drag Reduction*, Springer, New York, 155-185.

Luchik, T.S. and W.G. Tiederman, 1988, Turbulent structure in low-concentration drag-reducing channel flows, *J. Fluid Mech.* **190**, 241-263.

Lumley, G.L., 1969, Drag reduction by additives, *Ann. Rev. Fluid Mech.* **1**, 367-384.

L'vov, V.S., A. Pomyalov, I. Procaccia and V. Tiberkevich, 2004, Drag Reduction by Polymers in Wall Bounded Turbulence, *Phys. Rev. Letters* **92**, 244503 (4 pages).

Maulik, B.K., 1989, Numerical studies of the Oldroyd-B fluid stability and transition in planar channels, Ph. D Dissertation, Princeton University.

Min, T., J.Y. Yoo, H. Choi and D.D. Joseph, 2003, Drag reduction by polymer additives in a turbulent channel flow, *J. Fluid Mech.* **486**, 213-238.

Moin, P. and J. Kim, 1980, On the numerical solution of time-dependent viscous incompressible fluid flows involving solid boundaries, *J. Comp. Phys.* **35**, 381-392.

Mysels, K.J., 1949, Flow of thickened fluids, *U.S. Pattent* 2,492,173.

Orlandi, P., 1995, A tentative approach to the direct simulation of drag reduction by polymers, *J. Non-Newtonian Fluid Mech.* **60**, 277-301.

Orszag, S.A. and L.C. Kells, 1980, Transition to turbulence in plane Poiseuille and plane Couette Flow, *J. Fluid Mech.* **96**, 159-205.

Phillips, T.N. and I. M. Soliman, 1991, The influence matrix technique for the numerical spectral simulation of viscous incompressible flows, *Num. Meth. PDE* **7**, 9-24.

Ptasinski P.K., B.J. Boersma, F.T.M. Nieuwstadt, M.A. Hulsen, B.H.A.A. Van Den Brule and J.C.R. Hunt, 2003, Turbulent channel flow near maximum drag reduction: Simulations, experiments and mechanisms, *J. Fluid Mech.* **490**, 251-291.

Seyer, F.A. and A.M. Metzner, 1969, Turbulent in drag reducing systems, *A.I.Ch.E. J.* **15**, 426-434.

Sibilla S. and A. Baron, 2002, Polymer stress statistics in the near-wall turbulent flow of a drag-reducing solution, *Phys. Fluids* **14**, 1123-1136.

Sureshkumar, R. and A.N. Beris, 1995, Effect of artificial stress diffusivity on the stability of the numerical calculations and the flow dynamics of time-dependent viscoelastic flows, *J. Non-Newtonian Fluid Mech.* **60**, 53-80.

Sureshkumar, R., A.N. Beris and R.A. Handler, 1997, Direct numerical simulation of the turbulent channel flow of a polymer solution, *Phys. Fluids* **9**, 743-755.

Stone P.A., Roy A., Larson R.G. and Graham M.D., 2004, Polymer drag reduction in exact coherent structures of plane shear flow, *Phys. Fluids* **16**(9), 3470-3482.

Tanner, R.I., 2000, *Engineering Rheology*, 2nd Ed., Oxford University Press, Oxford.

Toms, B.A., 1949, Observations on the flow of linear polymer solutions through straight tubes at large Reynolds numbers, in: *Proc. Intl. Rheological Congress*, Holland 1948, North Holland, **2**, 135-141.

Van Heel, A.P.G., M.A. Hulsen and B.H.A.A. van den Brule,

1998, On the selection of parameters in the FENE-P model, *J. of Non-Newtonian Fluid Mech.* **75**, 253-271.

Virk, P.S., 1975, Drag reduction fundamentals, *A.I.Ch.E. J.* **21**, 625-656.

Vlachogiannis, M., M.W. Liberatore, A.J. McHugh and T.J. Hanratty, 2003, Effectiveness of a drag reducing polymer: Relation to molecular weight distribution and structuring, *Phys. Fluids* **15**, 3786-3794.

Wedgewood L.E. and R.B. BIRD, 1988, From molecular-models to the solution of flow problems, *Ind. & Eng. Chem. Res.* **27**(7), 1313-1320.

Yu, B. and Y. Kawaguchi, 2003, Effect of Weissenberg number on the flow structure: DNS study of drag-reducing flow with surfactant aditives, *Int. J. of Heat and Fluid Flow* **24**, 491-499.